Accepted Manuscript

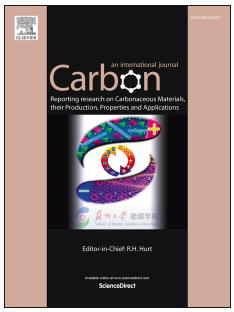

Understanding and manipulating luminescence in carbon nanodots

Z.C. Su, H.G. Ye, Z. Xiong, Q. Lou, Z. Zhang, F. Tang, J.Y. Tang, J.Y. Dai, C.X. Shan, S.J. Xu

PII: S0008-6223(17)31004-7

DOI: 10.1016/j.carbon.2017.10.013

Reference: CARBON 12450

To appear in: *Carbon*

Received Date: 22 August 2017

Revised Date: 23 September 2017

Accepted Date: 5 October 2017

Please cite this article as: Z.C. Su, H.G. Ye, Z. Xiong, Q. Lou, Z. Zhang, F. Tang, J.Y. Tang, J.Y. Dai, C.X. Shan, S.J. Xu, Understanding and manipulating luminescence in carbon nanodots, *Carbon* (2017), doi: 10.1016/j.carbon.2017.10.013.

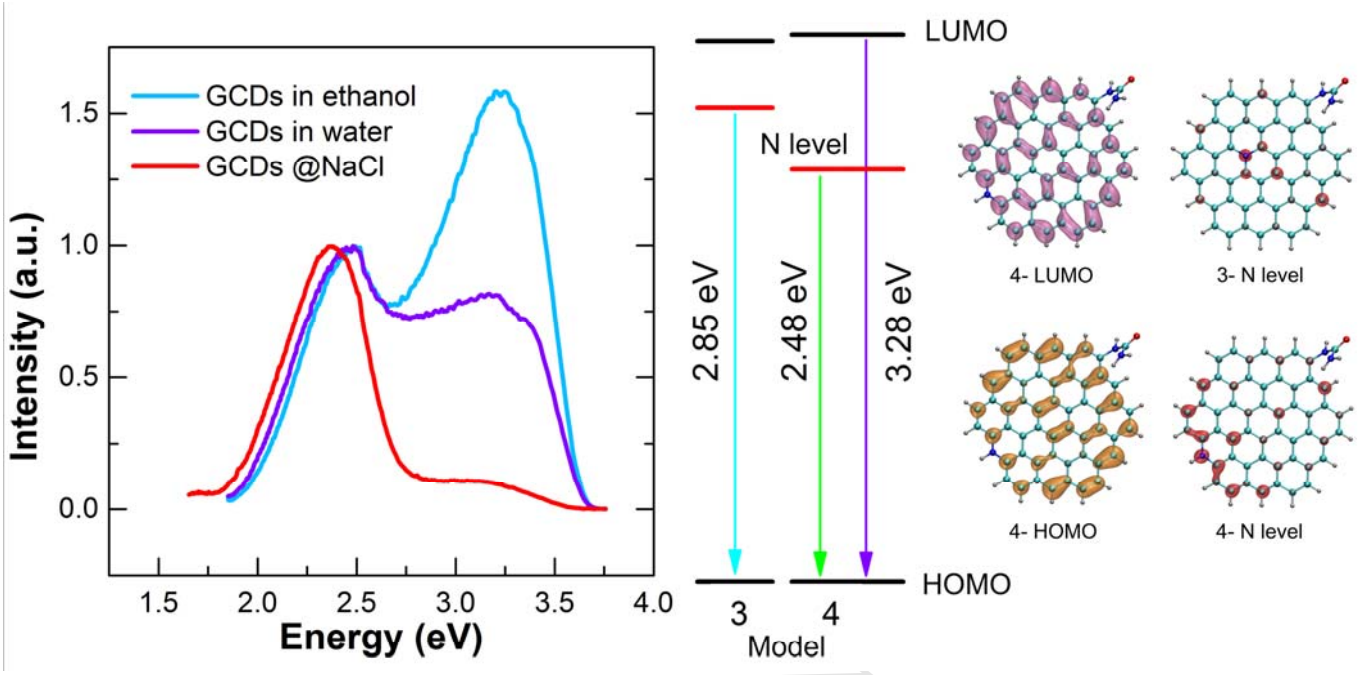

Understanding and Manipulating Luminescence in Carbon Nanodots

Z. C. Su,[1,#] H. G. Ye,[1, 2,#] Z. Xiong,[3] Q. Lou,[4] Z. Zhang,[5] F. Tang,[1] J. Y. Tang,[3] J. Y. Dai,[5] C. X. Shan,[4] and S. J. Xu[1*]

[1]Department of Physics, Shenzhen Institute of Research and Innovation (HKU-SIRI), and HKU-CAS Joint Laboratory on New Materials, The University of Hong Kong, Pokfulam Road, Hong Kong, China

[2]Department of Applied Physics, Xi'an Jiaotong University, Xi'an 710049, China

[3]Department of Chemistry, The University of Hong Kong, Pokfulam Road, Hong Kong, China

[4]School of Physics and Engineering, Zhengzhou University, Zhengzhou 450001, China

[5]Department of Applied Physics, Hong Kong Polytechnic University, Kowloon, Hong Kong, China

[#]These authors contributed equally to this work.

*Corresponding author. E-mail: sjxu@hku.hk (S. J. Xu)

Abstract

Carbon nanodots (CDs), a new star in the carbon nanomaterials family, have been demonstrated to show strong luminescence, and can meet the needs of large-scale production for biological and medical applications due to their low toxicity and biocompatibility. However, their luminescence mechanisms, such as color tuning and strong excitation-dependent luminescence, are still unclear. Herein, we present a state-of-the-art understanding and manipulating luminescence in CDs by changing their environmental states and using multiple spectroscopic methods as well as the first-

principles theoretical calculations. Our study reveals that the edge-carbon atoms and incorporated nitrogen atoms play critical roles in the luminescence mechanisms of CDs, and thus paves the way for manipulation of luminescence in CDs.

1. Introduction

Luminescent carbon nanodots (CDs) are a new star member in the family of carbon nanomaterials because they possess distinct advantages, such as multicolor emissions, photo stability, low toxicity, biocompatibility and feasible large-scale production.[1–6] Recently, CDs have attracted considerable interest due to their wide application potential in bioimaging, drug delivery, sensors, and light-emitting devices.[7–16] Still, their luminescence mechanisms, especially excitation wavelength dependent photoluminescence (PL) and self-quenching of luminescence in aggregated solid state, are unclear,[17–19] although a variety of models have been proposed to interpret the phenomena.[20–25]

In general, quantum confinement effect, surface traps and edge states are considered as the key factors in the luminescence mechanisms of CDs.[20,24] For size-dependent PL, the quantum confinement effect obviously plays a critical role, and has been firmly demonstrated by preparing CDs with different sizes. But, PL spectra of single CDs are found to be size independent.[4,26] On the other hand, continuous surface defect states have been suggested to be responsible for tunable emissions.[19,20,27] This widely adopted surface-defect model provides a good explanation to the excitation dependent luminescence. Very recently, distinct edge states induced by several carbon atoms on the lattice edge of CDs and so-called functional groups have been attributed to the physical origin of the common green emission of CDs and graphene quantum dots.[28] However, the edge state model seems difficult to interpret the largely tunable luminescence from blue to red commonly observed in CDs.[29]

The great application potential in a wide variety of fields and the lack of a deep insight into the luminescence mechanism jointly push us to conduct this study, in which we show that the defect states and edge states induced by the doped nitrogen atoms and carbon atoms on the edge of carbon sheet, respectively, act as luminescent centers for the colorful luminescence in CDs.

2. Experimental

2.1 Synthesis

The CDs were synthesized from urea and citric acid using microwave-assisted method. Detailed description on the synthesis procedures can be referred to previous studies.[13,30] Green and blue CDs were prepared from urea and citric acid in different mass ratios of 2:1 and 0.2:1, respectively. Then the CDs can be added into poly (vinyl alcohol) (PVA, J&K, average M.W.: 95000) aqueous solution (0.5 g PVA in 10 mL DI water), and dried for luminescent gel. The preparation method of incorporating green CDs into NaCl crystals was described elsewhere.[31]

2.2 Characterization

For the PL spectroscopic measurements, a home-assembled PL setup consisting of a Spex 750M monochromator and a Hamamatsu R928 photomultiplier detector was used. The 325 nm laser line of a Kimmon He-Cd laser was employed as the excitation light source in the steady-state PL spectral measurements. For the variable-temperature spectroscopic measurements, the samples were mounted on a cold finger of a Janis closed cycle cryostat providing a varying temperature range from 4 K to 300 K. Room-temperature IR spectra were registered on an IR Affinity-1 spectrophotometer. The excitation wavelength dependent spectroscopic measurements and TRPL decaying traces were obtained by using a spectrograph setup produced by Horiba PTI. The excitation light source was a 75 W Xe-lamp for the excitation wavelength dependent PL spectra. The

absorption spectrum was acquired as the ratio of two synchronous scanning with and without the sample in an integrating sphere. The TRPL signal was detected by using a laser strobe method under the excitation of a pulsed nitrogen laser whose emission wavelength was 337 nm, pulse width 800 ps, and repetition frequency 10 Hz. Transmission electron microscopy (TEM) images were recorded with a FEI-TECNAI G2 F30 transmission electron microscope operating at 200 kV.

2.3 Theoretical calculations

The first-principles calculations based on the density functional theory were carried out using the Vienna ab initio simulation package (VASP) code.[32,33] The generalized gradient approximation is used for exchange correlation.[34] The interaction between core and valence electrons are treated with the projector augmented wave method.[35] The energy cutoff for the plane wave basis function is 400 eV. Only the Γ point was employed for the Monkhorst-Pack k-point mesh. The supercell to simulate the carbon quantum dot was in size of 25Å×25Å×10Å including 54 carbon atoms and a NH_2CONH_2 group. The dangling bonds on the edge of carbon sheet were saturated by hydrogen atoms. The nitrogen impurity was formed by replacing a carbon atom with a nitrogen atom. All of the atoms in the model were allowed to relax freely by minimizing the quantum mechanical force on each ion to be less than 0.03 eV/Å.

3. Results and discussion

First of all, aggregation-induced luminescence quenching in solid state could be a severe problem hindering application of CDs. Two kinds of CDs, namely green and blue CDs (hereafter denoted as GCDs and BCDs), were produced by one-step microwave synthesis route. As shown in Fig. 1(a), green CDs only demonstrated strong photoluminescence when they dissolved in some solution (e.g. liquid ethanol) under the excitation of a 405

nm laser. The intense luminescence quickly quenched as the ethanol evaporated. This phenomenon was termed aggregation-induced luminescence quenching in solid state.[18,36] In order to avoid luminescence quenching induced by solid-state aggregation, the CDs are usually dispersed into a polymer matrix, or glued on the surface of other particles.[17,37] For example, as shown in Fig. 1(b), the green CDs were dispersed in poly(vinyl alcohol) (PVA) solution and then painted on a glass substrate. Dried gel containing CDs still exhibits strong green luminescence under the excitation of a 405 nm laser. From HRTEM images of the green CDs shown in Figs. 1(c) and 1(d), CDs with well-resolved lattice structures in the core can be seen. Parallel lattice fringes with an interplanar spacing of 0.21 nm shall be associated with the (100) facet of graphitic carbon.[9,15] Close relationship between the luminescent CDs and graphene quantum dots was claimed by different groups.[14,15,19,28] Furthermore, full-color light-emitting carbon dots have also been achieved by Ding *et al*. via surface engineering.[29]

Figs. 1(e) and 1(f) show TEM images of the green and blue CDs, respectively. The insets give statistic size distributions of GCDs and BCDs. It can be seen that most (about 85% for GCDs, 87% for BCDs) of the CDs falls within the scope of 2.0-3.0 nm. The average size is 2.36 nm and 2.34 nm for GCDs and BCDs, respectively. Evidently, there is no significant difference in particle size between the green and blue CDs. Thus the quantum confinement effect seems not the mechanism of different emissions for the GCDs and BCDs samples in this study, which is consistent with single-particle spectroscopic measurements.[26] Herein, we concentrate on the interpretation of luminescence mechanisms in CDs, as argued below.

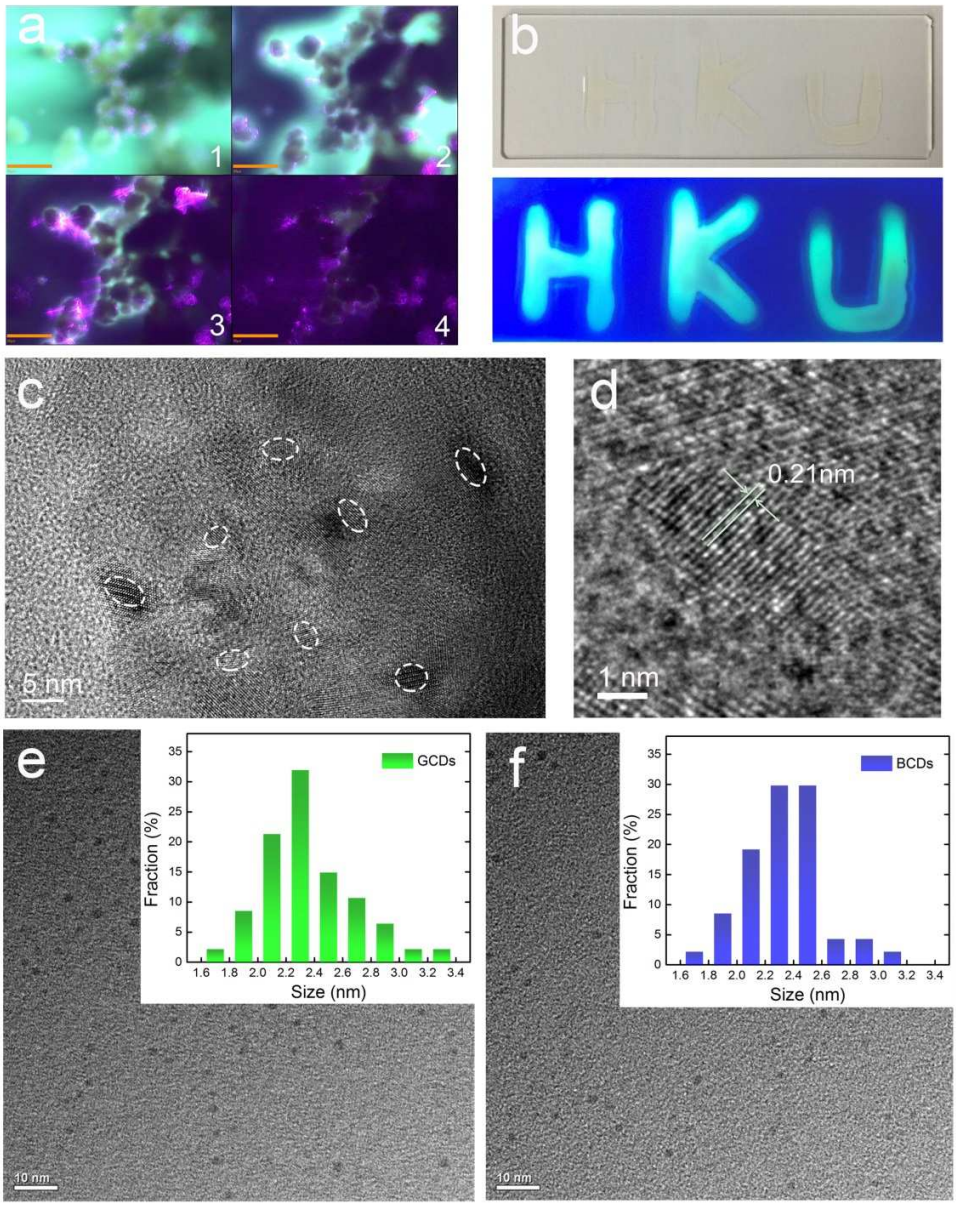

Figure 1. (a) Optical images of green CDs dissolved in ethanol solution under the excitation of a 405 nm laser at room temperature. Green luminescence quenching can be seen as the evaporation of ethanol occurs (From 1 to 4). The scale bar is 80 μm in the photographs. (b) Photographs of green CDs dispersed in PVA in solid state on a glass substrate under the illumination of the sunlight (upper) and a 405 nm laser (bottom), respectively, at room temperature. (c) and (d) HRTEM images of green CDs. The scale

bars in (c) and (d) are 5 nm and 1 nm, respectively. TEM images and size distributions of (e) green CDs and (f) blue CDs. The scale bars in (e) and (f) are 10 nm.

Another luminescence characteristic of CDs is excitation-dependent photoluminescence property. Shown in Figs. 2(a) and 2(b) are the excitation-wavelength dependent PL spectra of the GCDs and BCDs dispersed in ethanol solution. Actually, two emission bands were observed in the PL spectra of the GCDs. One is located at about 500 nm, while the other located at 350 nm for the sample excited by an ultraviolet 325 nm laser. Measured UV-vis absorption spectra (solid lines) in Fig. 2(c) also indicate that an absorption peak at ~325 nm occurs for the green CDs. For the BCDs, the broad emission band is located at about 450 nm. In fact, a shoulder at about 500 nm can be also resolved in the room-temperature PL spectrum of the blue CDs in ethanol solution, as shown in Fig. 3(a). The excitation-dependent photoluminescence is resulted from the very broad emission bands which may be induced by dopant fluctuation and size distribution of the CDs samples.[24] Partial excitation of the bands can be achieved by longer wavelengths and corresponding emission would be observed. This feature of CDs enhances the biomedical applications in the near infrared region.[11] Time-resolved PL decay curves of the two samples were also measured at the respective emission peak, as plotted in Fig. 2(d). With the single exponential decay function derived in ref. 38, PL lifetime of 22.4 ns (17.5 ns) were determined for the green (blue) CDs.[38] From room-temperature PL spectra shown in Figs. 3(a) and 3(b), it can be evidently seen that the luminescence spectral characteristics of both the green and blue CDs show a strong dependence on the solution type and thus surrounding environment. For example, in the ethanol solution, GCDs and BGDs show very dissimilar emission spectra when they were illuminated by the 325 nm laser. Surprisingly, both GCDs and BCDs produce blue PL spectra in the acetone solution with very similar spectral features. A weak shoulder at 500 nm was observed in the two PL spectra. Actually, UV laser induced chemical reaction was observed in the acetone solution with green CDs under the illumination of 325 nm UV laser. As seen in Fig. 3(d), convection phenomenon occurred in the acetone solution in

the quartz tube under the illumination of 325 nm UV laser. More interestingly, bottom illuminated part of the solution tube exhibits green emission, while upper illuminated part of the solution shows blue emission, in spite of both parts illuminated by the same 405 nm laser (see Figs. 3(e) and 3(f)).

The occurrence of UV laser induced chemical reaction gives us a hint about the key role of surface functional groups (i.e., defects) in luminescence of the CDs. And even the green CDs can be surface engineered to generate blue emission. In fact, pH value of solution was reported to have a significant influence on PL from CDs by Hao *et al*.[23] As the CDs studied here were synthesized from carbonization of urea and citric acid, the surface functional groups mainly include $CONH_2$, COOH and OH. To test the existence of these surface functional groups, infrared absorption spectra of CDs were measured and shown in Fig. 4(d). As expected, the absorption spectra of both the CDs show evident spectral structures of the functional molecular groups. Nevertheless, the infrared absorption spectrum of the green CDs exhibits an additional absorption peak at about 1100 cm^{-1}, which corresponds to the signal of C-N stretching vibrations. Another difference between the two absorption spectra shall be vibrational bands of C=O in 1600-1800 cm^{-1}.[28] These absorption bands become relatively stronger in the green CDs sample, which is expected because more urea (NH_2CONH_2) was used in the synthesis of the green CDs.[13]

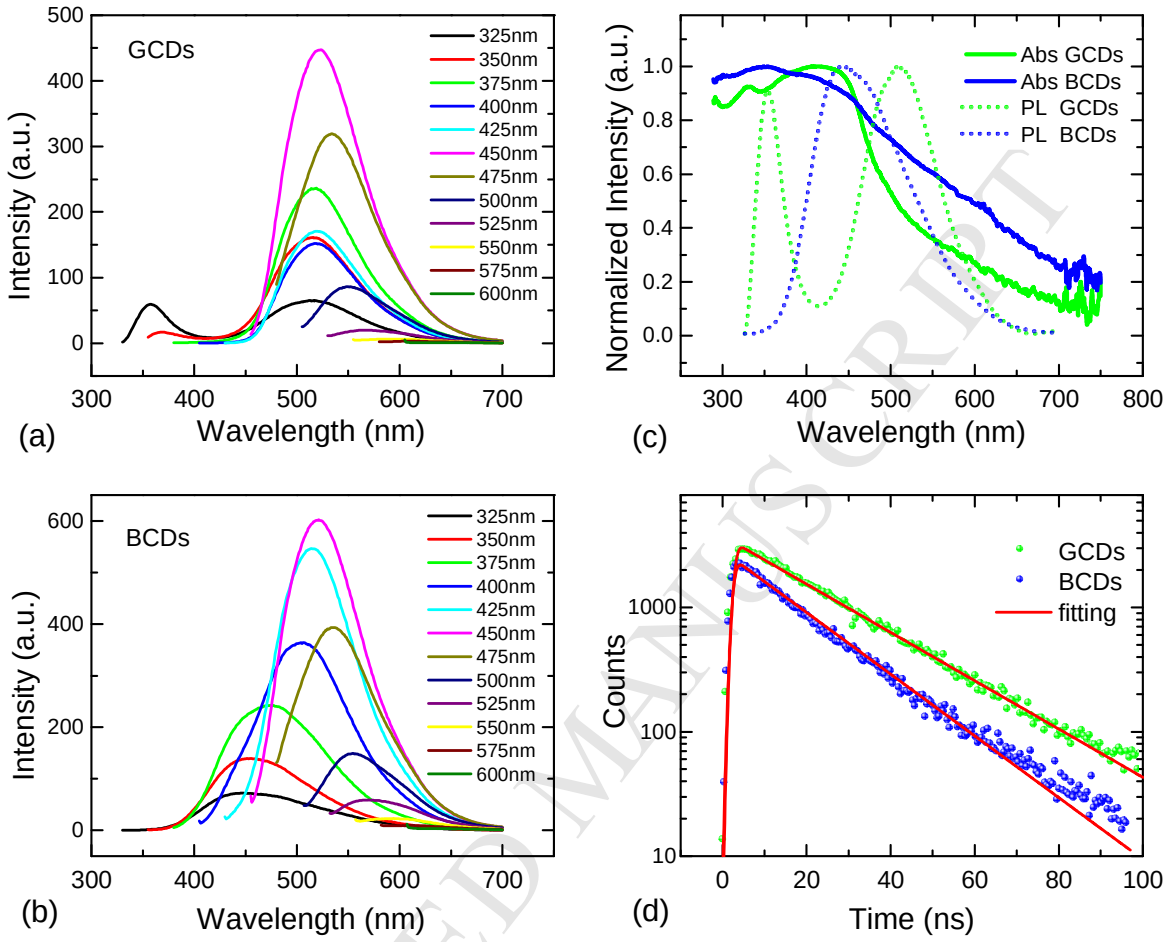

Figure 2. Excitation-wavelength dependent PL spectra of (a) green and (b) blue CDs in ethanol solution at room temperature. (c) Normalized UV-vis absorption spectra (solid lines) and PL spectra (dotted lines. Under the 325 nm laser excitation) of green and blue nanodots in ethanol solution. (d) Time-resolved PL decay curves of green and blue nanodots in ethanol solution. The red solid lines are the fitting curves with the model decay function derived in Ref. 38.

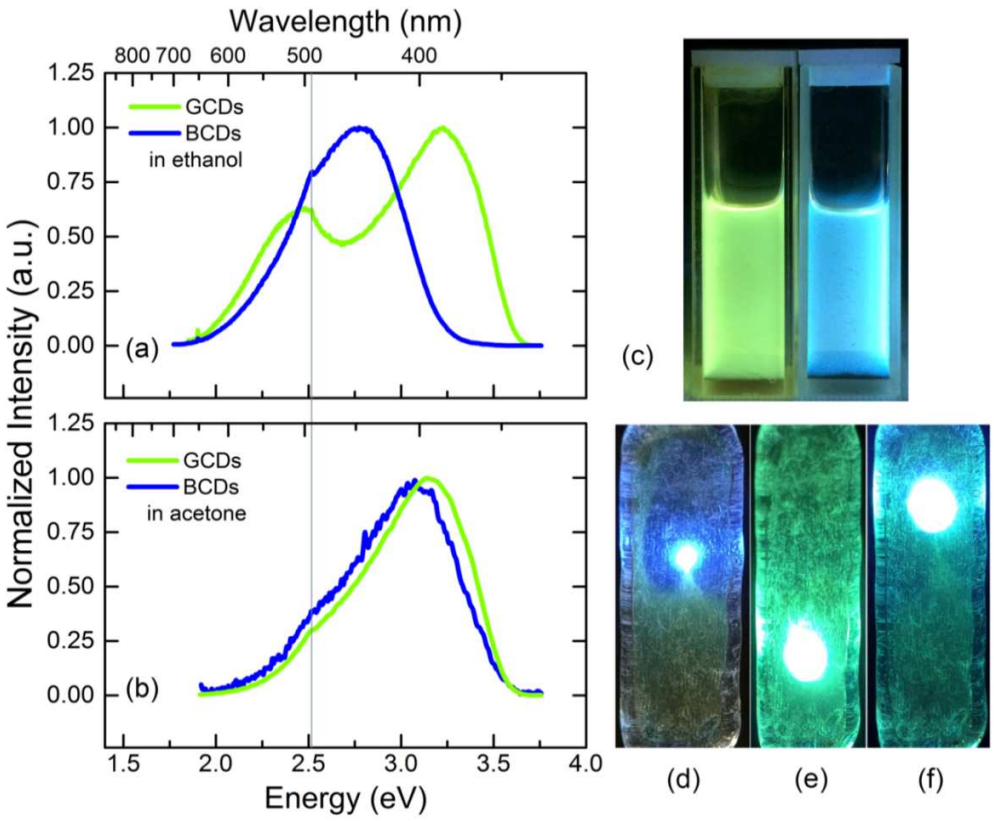

Figure 3. Room-temperature PL spectra of the CDs dispersed in (a) ethanol and (b) acetone solutions under the excitation of 325 nm UV laser. (c) Fluorescence images of the green (left) and blue (right) nanodots in ethanol solution under the illumination of an UV lamp. (d) Photograph of the green nanodots in acetone solution under the 325 nm laser excitation. (e) and (f) Photographs of the green nanodots in acetone solution under the 405 nm laser excitation for bottom and upper part of the solution, respectively. The bottom illuminated part shows green emission (e), while the upper part shows blue emission (f).

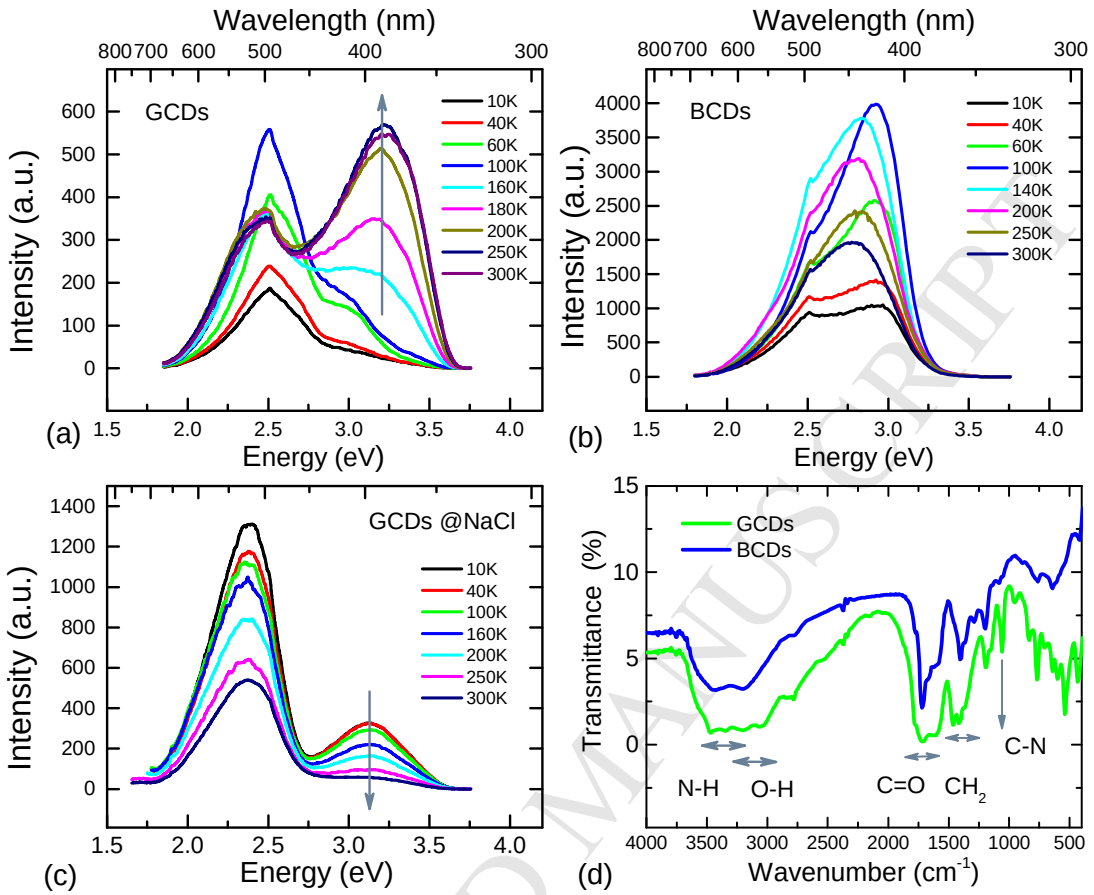

Figure 4. Temperature-dependent PL spectra of the (a) green CDs in ethanol solution, (b) blue CDs in ethanol solution, and (c) green nanodots incorporated into NaCl crystal. (d) Infrared absorption spectra of the CDs powders at room temperature.

To further investigate the luminescence mechanisms of the CDs, variable-temperature PL measurements were conducted under the excitation of UV 325 nm laser. Temperature-dependent PL spectra of the green and blue CDs in ethanol solution are depicted in Figs. 4(a) and 4(b), respectively. Clearly, distinct PL spectra consisting of double main structures were observed for the two samples. But, the PL spectra of the two samples show different evolution behaviors with temperature. For the green CDs in ethanol

solution, the emission band located at shorter wavelength shows a strong temperature induced enhancement in the range of 100-250 K, as indicated by an upward arrow in the figure. The spectral structure located at 500 nm displays a fast increase with temperature in the range of 40-100 K. Note that ethanol has a melting point of about 160 K. These results may suggest that the two luminescence bands most likely have different origins. For the blue CDs, the PL intensity increases with increasing the temperature in the range of 10-100 K, and turned to decrease for temperatures beyond 100 K. It shall be noted that the PL intensity of both CDs in ethanol solution reaches its respective minimum value at 10 K.

For a comparative study, the green nanodots were incorporated into NaCl crystal, and then variable-temperature PL spectra of the composite sample were and measured. The PL results are illustrated in Fig. 4(c). Again, the two emission bands were well resolved in the PL spectra. In sharp contrast to the cases of solution samples, the emission intensity of the solid composite sample monotonically decreases with increasing the temperature, so that the band peaking at ~380 nm almost quenches at 300 K. The results again indicate that the surrounding environment has a decisive impact on luminescence of CDs. To further strengthen this concluding point, room-temperature PL spectra of the green CDs on different surrounding environments (i.e., in water, ethanol solution and solid NaCl crystal) were shown in Fig. 5. Note that all the PL spectra were normalized at the longer wavelength peak just for clear comparison. Because of the more sensitivity of the emission band at 380 nm on the external environment, it is reasonable for one to believe that this band more likely originates from surface states than the 500 nm band for the green CDs.

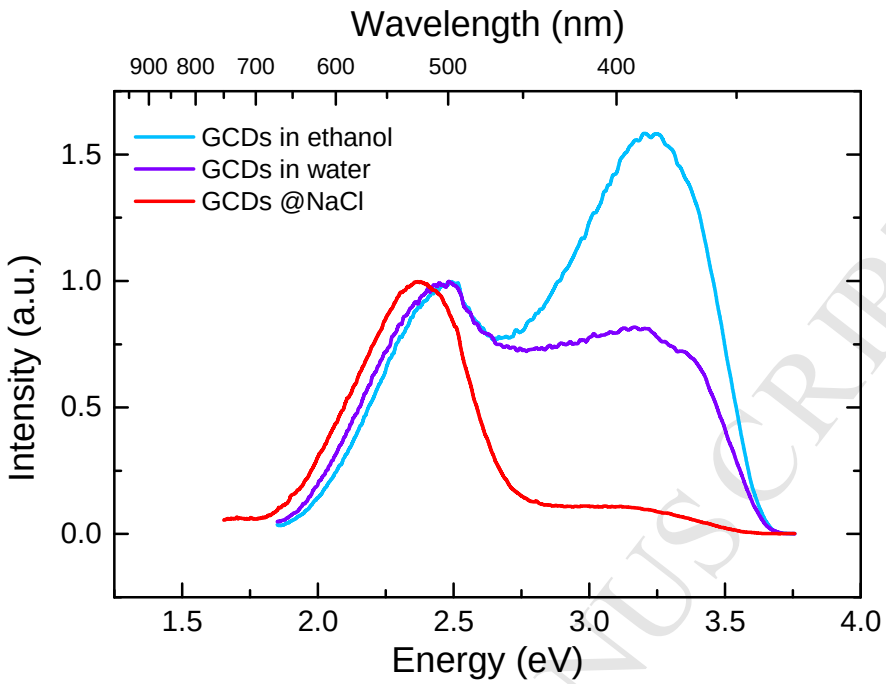

Figure 5. Room-temperature PL spectra of the green CDs in ethanol solution, aqueous solution, and incorporated into NaCl crystal. Note that all the PL spectra were normalized at the longer wavelength peak just for clear comparison.

To have a deeper insight into the luminescence mechanisms, we performed the first-principles calculations on the electronic structures of CDs with various possible configurations. Through a large amount of calculations, the surface functional groups and doped nitrogen are eventually selected and concentrated, as shown and argued below.

There have been a lot of studies showing that CDs are small pieces of graphene sheets.[15][26][28] Some CDs were even directly fabricated from exfoliation of large graphite with top-down approach.[8][24] In first-principles calculations, doped graphene sheets are widely used as CDs model.[15][25][39] We thus start the first-principles calculations from a hydrogenated monolayer graphene sheet consisting of 54 carbon atoms (Model 1). And then a NH_2CONH_2 group of urea is connected with the edge of

Model 1 to form Model 2. Then Model 3 and 4 are calculated by doping a nitrogen atom into the sheet center and at the sheet edge, respectively. The calculated energy eigenvalues near the fermi level are illustrated in Fig. 6. The energy band gap here is defined as the separation between the intrinsic HOMO and LUMO of graphite sheet and the level between them is identified as defect level. From the energy level diagram in Fig. 6, we can see that the bandgap keep almost unchanged from Model 1 to Model 4. Due to the well-known band gap underestimation of the first-principles calculation, the firsthand energy gap (1.902, 1.861, 1.906, 1.928 eV for Model 1 to 4) was manually matched with the experimental value of 3.28 eV according to Model 4, so that effective comparison with experiment can be done. The contact of NH_2CONH_2 group, as well as COOH and OH, does not introduce any energy level in the band gap, so their influence on the photoluminescence property can be excluded. The defect level in the band gap of model 3 and 4 is from the substitutional nitrogen atom. Its position is sensitive to the site of dopant. To support our identification to these energy levels, the charge density distributions of LUMO, HOMO and nitrogen induced defect levels are shown in the right panel of Fig. 6. The LUMO and HOMO are much extended state covering the whole graphite sheet. However, for the nitrogen dopant induced energy levels, the charge distributions are strongly localized near the nitrogen atoms and the edge-carbon atoms in Model 3 and 4, respectively. Energy separations between the nitrogen induced levels and the HOMO level are found to be 2.85 eV and 2.48 eV in Model 3 and 4, respectively. These energy values are highly consistent with the emission bands at 440 nm of BCDs and 500 nm of GCDs, respectively.

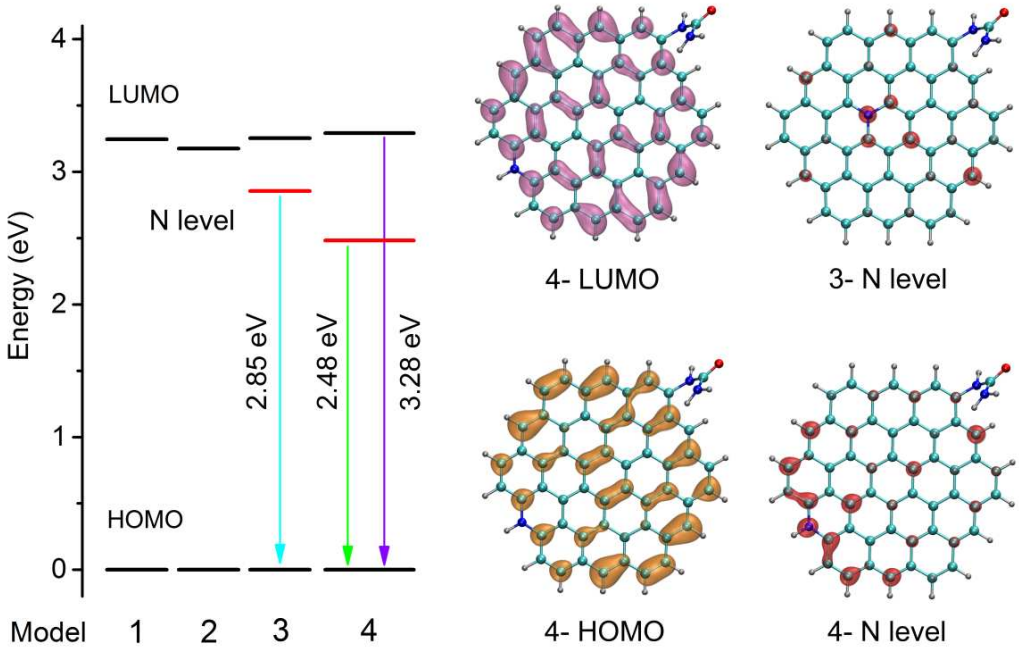

Figure 6. Calculated energy levels and charge density distribution of LUMO, HOMO and N induced level of different models.

Based on above discussions, we propose a three-level schematic picture for the luminescence of carbon nanodots. The carbon sheets provide delocalized and unified HOMO and LUMO levels, while N dopants act as localized luminescent centers lying in between the HOMO and LUMO levels. Different N atom incorporation positions and even numbers would significantly affect the defect levels, which in turn results in different color emissions of carbon nanodots. The carbon atoms on the edge of graphene sheet play important roles in HOMO and LUMO, as well as N dopants induced levels. Thus the emission of carbon nanodots, especially the UV emission of HOMO and LUMO, is very sensitive to the external environment. And aggregation-induced luminescence quenching could be explained by the influence of edge states.

4. Conclusions

A systematic study has been carried out for elucidating the luminescence mechanisms of CDs. The influences of various surrounding circumstances, surface functional groups, and doped nitrogen atoms on the luminescence of CDs have been particularly investigated. The edge states predominantly induced by carbon atoms on the edge of graphene sheet and doped nitrogen atoms are believed to play key roles in the environment-sensitive luminescence of CDs.

Acknowledgments

The study was financially supported by Natural Science Foundation of China (Grant No. 11374247), and in part by the SRT on New Materials of HKU, as well as HK-UGC AoE Grants (Project No.: AoE/P-03/08). Z.Z. and J.Y.D. are grateful to financial support of Hong Kong PolyU Postdoc Fellow Grant (No: 1-YW0A).

One of the authors, Z.C.S., wishes to thank Mr. Yunhao Zheng for his assistance in preparing the quartz colorimetric tubes used for the variable-temperature spectroscopic measurements and Ms. Qian Li for her assistance in the IR spectral measurements.

References

[1] L. Zheng, Y. Chi, Y. Dong, J. Lin, B. Wang, Electrochemiluminescence of water-soluble carbon nanocrystals released electrochemically from graphite, J. Am. Chem. Soc. 131 (2009) 4564–4565.

[2] H. Zhu, X. Wang, Y. Li, Z. Wang, F. Yang, X. Yang, Microwave synthesis of

fluorescent carbon nanoparticles with electrochemiluminescence properties., Chem. Commun. 34 (2009) 5118–20.

[3] S.N. Baker, G.A. Baker, Luminescent carbon nanodots: Emergent nanolights, Angew. Chemie - Int. Ed. 49 (2010) 6726–6744.

[4] H. Li, X. He, Z. Kang, H. Huang, Y. Liu, J. Liu, et al., Water-soluble fluorescent carbon quantum dots and photocatalyst design, Angew. Chemie - Int. Ed. 49 (2010) 4430–4434.

[5] L. Bao, Z.L. Zhang, Z.Q. Tian, L. Zhang, C. Liu, Y. Lin, et al., Electrochemical tuning of luminescent carbon nanodots: From preparation to luminescence mechanism, Adv. Mater. 23 (2011) 5801–5806.

[6] X. Zhai, P. Zhang, C. Liu, T. Bai, W. Li, L. Dai, et al., Highly luminescent carbon nanodots by microwave-assisted pyrolysis, Chem. Commun. 48 (2012) 7955–7957.

[7] P. Gong, Z. Yang, W. Hong, Z. Wang, K. Hou, J. Wang, et al., To lose is to gain: Effective synthesis of water-soluble graphene fluoroxide quantum dots by sacrificing certain fluorine atoms from exfoliated fluorinated graphene, Carbon 83 (2015) 152–161.

[8] J. Wang, C.-F. Wang, S. Chen, Amphiphilic Egg-Derived Carbon Dots: Rapid Plasma Fabrication, Pyrolysis Process, and Multicolor Printing Patterns, Angew. Chemie. 124 (2012) 9431–9435.

[9] P. Gong, J. Wang, K. Hou, Z. Yang, Z. Wang, Z. Liu, et al., Small but strong: The influence of fluorine atoms on formation and performance of graphene quantum dots using a gradient F-sacrifice strategy, Carbon 112 (2017) 63–71.

[10] S. Zhu, Q. Meng, L. Wang, J. Zhang, Y. Song, H. Jin, et al., Highly photoluminescent carbon dots for multicolor patterning, sensors, and bioimaging, Angew. Chemie - Int. Ed. 52 (2013) 3953–3957.

[11] J. Tang, B. Kong, H. Wu, M. Xu, Y. Wang, Y. Wang, et al., Carbon nanodots featuring efficient FRET for real-time monitoring of drug delivery and two-photon imaging, Adv. Mater. 25 (2013) 6569–6574.

[12] W. Kwon, S. Do, J. Lee, S. Hwang, J.K. Kim, S.W. Rhee, Freestanding luminescent films of nitrogen-rich carbon nanodots toward large-scale phosphor-based white-light-emitting devices, Chem. Mater. 25 (2013) 1893–1899.

[13] S. Qu, X. Liu, X. Guo, M. Chu, L. Zhang, D. Shen, Amplified spontaneous green emission and lasing emission from carbon nanoparticles, Adv. Funct. Mater. 24 (2014) 2689–2695.

[14] P. Innocenzi, L. Malfatti, D. Carboni, Graphene and carbon nanodots in mesoporous materials: an interactive platform for functional applications, Nanoscale. 7 (2015) 12759–12772.

[15] X. Li, M. Rui, J. Song, Z. Shen, H. Zeng, Carbon and Graphene Quantum Dots for Optoelectronic and Energy Devices: A Review, Adv. Funct. Mater. 25 (2015) 4929–4947.

[16] W. Liu, C. Li, Y. Ren, X. Sun, W. Pan, Y. Li, et al., Carbon dots: surface engineering and applications, J. Mater. Chem. B. 4 (2016) 5772–5788.

[17] M. Sun, S. Qu, Z. Hao, W. Ji, P. Jing, H. Zhang, et al., Towards efficient solid-state photoluminescence based on carbon-nanodots and starch composites, Nanoscale. 6 (2014) 13076–13081.

[18] Q. Lou, S. Qu, P. Jing, W. Ji, D. Li, J. Cao, et al., Water-triggered luminescent “nano-bombs” based on Supra-(carbon nanodots), Adv. Mater. 27 (2015) 1389–1394.

[19] S. Zhu, Y. Song, X. Zhao, J. Shao, J. Zhang, B. Yang, The photoluminescence mechanism in carbon dots (graphene quantum dots, carbon nanodots, and polymer

dots): current state and future perspective, Nano Res. 8 (2015) 355–381.

[20] S. Zhu, J. Zhang, S. Tang, C. Qiao, L. Wang, H. Wang, et al., Surface chemistry routes to modulate the photoluminescence of graphene quantum dots: From fluorescence mechanism to up-conversion bioimaging applications, Adv. Funct. Mater. 22 (2012) 4732–4740.

[21] S. Ghosh, A.M. Chizhik, N. Karedla, M.O. Dekaliuk, I. Gregor, H. Schuhmann, et al., Photoluminescence of carbon nanodots: Dipole emission centers and electron-phonon coupling, Nano Lett. 14 (2014) 5656–5661.

[22] V. Nguyen, J. Si, L. Yan, X. Hou, Electron-hole recombination dynamics in carbon nanodots, Carbon 95 (2015) 659–663.

[23] Y. Hao, Z. Gan, X. Zhu, T. Li, X. Wu, P.K. Chu, Emission from trions in carbon quantum dots, J. Phys. Chem. C. 119 (2015) 2956–2962.

[24] Z. Gan, H. Xu, Y. Hao, Mechanism for excitation-dependent photoluminescence from graphene quantum dots and other graphene oxide derivates: consensus, debates and challenges, Nanoscale. 8 (2016) 7794–7807.

[25] P. Jing, D. Han, D. Li, D. Zhou, L. Zhang, H. Zhang, et al., Origin of Anisotropic Photoluminescence in Heteroatom-Doped Carbon Nanodots, Adv. Opt. Mater. 5 (2017) 1601049.

[26] Q. Xu, Q. Zhou, Z. Hua, Q. Xue, C. Zhang, X. Wang, et al., Single-Particle Spectroscopic Measurements of Fluorescent Graphene Quantum Dots, ACS Nano. 7 (2013) 10654–10661.

[27] V. Nguyen, J. Si, L. Yan, X. Hou, Direct demonstration of photoluminescence originated from surface functional groups in carbon nanodots, Carbon 108 (2016) 268–273.

[28] L. Wang, S.J. Zhu, H.Y. Wang, S.N. Qu, Y.L. Zhang, J.H. Zhang, et al., Common

origin of green luminescence in carbon nanodots and graphene quantum dots, ACS Nano. 8 (2014) 2541–2547.

[29] H. Ding, S. B. Yu, J. S. Wei, H. M. Xiong, Full-color light-emitting carbon dots with a surface-state-controlled luminescence mechanism, ACS Nano. 10 (2016) 484–491.

[30] S. Qu, X. Wang, Q. Lu, X. Liu, L. Wang, A biocompatible fluorescent ink based on water-soluble luminescent carbon nanodots, Angew. Chemie - Int. Ed. 51 (2012) 12215–12218.

[31] Y. Zhai, D. Zhou, P. Jing, D. Li, H. Zeng, S. Qu, Preparation and application of carbon-nanodot@NaCl composite phosphors with strong green emission, J. Colloid Interface Sci. 497 (2017) 165–171.

[32] G. Kresse, J. Furthmüller, Efficiency of ab-initio total energy calculations for metals and semiconductors using a plane-wave basis set, Comput. Mater. Sci. 6 (1996) 15–50.

[33] G. Kresse, J. Furthmüller, Efficient iterative schemes for ab initio total-energy calculations using a plane-wave basis set, Phys. Rev. B. 54 (1996) 11169–11186.

[34] J. P. Perdew, Y. Wang, Accurate and simple analytic representation of the electron-gas correlation energy, Phys. Rev. B. 45 (1992) 13244–13249.

[35] G. Kresse, D. Joubert, From ultrasoft pseudopotentials to the projector augmented-wave method, Phys. Rev. B. 59 (1999) 1758–1775.

[36] D.-Y. Guo, C.-X. Shan, K.-K. Liu, Q. Lou, D.-Z. Shen, Surface plasmon effect of carbon nanodots, Nanoscale. 7 (2015) 18908–18913.

[37] D. Zhou, Y. Zhai, S. Qu, D. Li, P. Jing, W. Ji, et al., Electrostatic Assembly Guided Synthesis of Highly Luminescent Carbon-Nanodots@$BaSO_4$ Hybrid Phosphors with Improved Stability, Small. 13 (2017) 1602055.

[38] Z. C. Su, S. J. Xu, A generalized model for time-resolved luminescence of localized carriers and applications: Dispersive thermodynamics of localized carriers, Sci. Rep. 7 (2017) 13.

[39] P. Gong, J. Wang, W. Sun, D. Wu, Z. Wang, Z. Fan, et al., Tunable photoluminescence and spectrum split from fluorinated to hydroxylated graphene, Nanoscale. 6 (2014) 3316-3324.